OD LOCALIZATION USING VESSEL BASED IMAGE ORIENTATION INDEPENDENT APPROACHES

BY

BODEETORN SUTCHARIT

A THESIS SUBMITTED IN PARTIAL FULFILLMENT OF THE REQUIREMENTS FOR THE DEGREE OF MASTER OF ENGINEERING (INFORMATION AND COMMUNICATION TECHNOLOGY FOR EMBEDDED SYSTEMS) SIRINDHORN INTERNATIONAL INSTITUTE OF TECHNOLOGY THAMMASAT UNIVERSITY

ACADEMIC YEAR 2017

OD LOCALIZATION USING VESSEL BASED IMAGE ORIENTATION INDEPENDENT APPROACHES

BY

BODEETORN SUTCHARIT

A THESIS SUBMITTED IN PARTIAL FULFILLMENT OF THE REQUIREMENTS FOR THE DEGREE OF MASTER OF ENGINEERING (INFORMATION AND COMMUNICATION TECHNOLOGY FOR EMBEDDED SYSTEMS) SIRINDHORN INTERNATIONAL INSTITUTE OF TECHNOLOGY THAMMASAT UNIVERSITY ACADEMIC YEAR 2017

OD LOCALIZATION USING VESSEL BASED IMAGE ORIENTATION INDEPENDENT APPROACHES

A Thesis Presented

By

BODEETORN SUTCHARIT

Submitted to

Sirindhorn International Institute of Technology

Thammasat University

In partial fulfillment of the requirements for the degree of

MASTER OF ENGINEERING (INFORMATION AND COMMUNICATION TECHNOLOGY FOR EMBEDDED SYSTEMS)

Approved as to style and content by

Advisor	P. Aimmanee (Asst. Prof. Dr. Pakinee Aimmanee)
Committee Member and Chairperson of Examination Committee	(Dr. Duangrat Gansawat)
Committee Member	(Prof. Dr. Stanislav S. Makhanov)
Committee Member	(Prof. Dr. Hirohiko Kaneko)

JULY 2018

Acknowledgements

Foremost, I would like to express my sincere gratitude to my advisor Asst. Prof. Pakinee Aimmanee for the continuous support of my master degree study and research. Her guidance helped me in all the time of research and writing of this thesis. Over the past two years, it has been a valuable time working under her guidance.

Besides my advisor, I would like to thank the rest of my thesis committee: Prof. Dr. Stanislav S. Makhanov, chairperson of examination committee from Sirindhorn International Institute of Technology (SIIT), Dr. Duangrat Gansawat, thesis committee from National Electronics and Computer Technology Center (NECTEC), and Prof. Dr. Hirohiko Kaneko, thesis committee from Tokyo Institute of Technology (Tokyo-Tech), for their encouragement, insightful comments and feedbacks to make this work better.

I would like to thank Prof. Dr. Thanaruk Theeramunkong, the head of the school. He had introduced me about this master degree program when I was an undergraduate student. Finally, I would like to thank my institute, Sirindhorn International Institute of Technology (SIIT), Thammasat University (TU) for financial support.

Abstract

OD LOCALIZATION USING VESSEL BASED IMAGE ORIENTATION INDEPENDENT APPROACHES

by

BODEETORN SUTCHARIT

Master of Science, Sirindhorn International Institute of Technology, 2016

Master of Engineering, Sirindhorn International Institute of Technology, 2018

Automatic Optic Disc (OD) localization is an essential problem in ophthalmic image processing. Knowing its location not only helps doctors with the early detection of sight threatening diseases but provide early diagnostic solutions for patient. With the existing methods, there are limitations on computation time and disorientated image cases. Many algorithms fail to locate the OD if the input image is tilted by a certain degree. This thesis presents two machine learning methods which mainly rely on information from retinal vessel network.

The first method is called Rotational 2D Vessel Projection with Decision Tree Classification which is an improved version of the Rotational 2D Vessel Projection (RVP). The Mahfouz's et al. approach with decision tree classification is applied on to a sequence of rotated images to find the most overlapped area of the OD candidates return from each round of iteration. The proposed method has been tested on different starting angles between 0 to 180 degrees from STARE and ROP datasets. We achieved an average accuracy of 85% and 79% for ROP.

The second method is called circular Hough transform with KNN classification (CH-KNN) which predicts and fills the curvature of the thick vessels using circular shape. With the help of Hough transform and KNN classification, the proposed method achieved a higher accuracy of 87% for STARE and 80% for ROP datasets.

Keywords: Classification, OD, Rotation, Vessel Projection

Table of Contents

List of Tables

Tables **Page**

List of Figures

Chapter 1
Introduction

1.1 Background

1.1.1 Optic Disc

The retina is a complex layer of tissue positioned near the optic nerve. Its function is to receive and relay light to the brain in order for us to visualize images. The zone where major blood vessels combine into the brain is called the Optic Disc (OD). Alternately, the OD can also be called an optic nerve head which can be seen in Fig. 1. The appearance of OD in normal fundus image is as a circular bright object. The OD contains no photoreceptors and, therefore, can be referred to as a blind spot. A digital fundus camera can be used to view the OD as well as other interior structures of the eye.

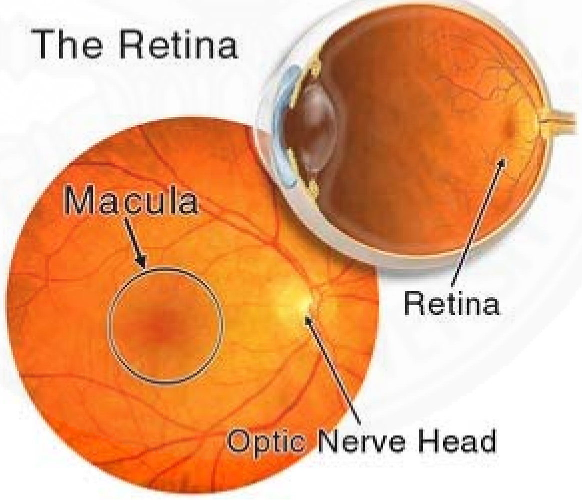

Figure 1.1 Fundus components

To help the doctor in retinal analysis, several automatic OD detection techniques are being proposed. OD localization is crucial in optical image analysis. Not only does it helps in forming a frame of reference within the eye toward locating other retina components such as the fovea and macula but also helps in retinal vessels tracking and segmentation. These factors can be combined to assist doctors in determining eye diseases such as glaucoma and hypertensive retinopathy. Glaucoma is an eye condition which damages the internal structures of the eye as well as the optic disc. It usually occurs when the fluid builds up inside the eye and causes the intraocular pressure to increase.

The methods of OD localization can be seen as two categories [3]. One of them is called appearance-based method which focuses on the OD features such as its intensity and shape. This category utilizes methods such as intensity thresholding, average variation, principle component analysis, and matched spatial filter to use against normal fundus image. These methods are still susceptible to diseased retinal image and can lead to incorrect OD location. Another category is called model-based method which focuses on the blood vessels extraction. In this work, we define the OD region to be the location where the blood vessels originated from. To increase the accuracy, our proposed method utilized features from both categories.

1.2 Problem statement

One common problem we face with automatic OD localization is the time it takes to process large number of images. Some existing techniques have complicate procedures that consume large computation time. Orientation of the image must also be fixed with most existing techniques. While this is not the problem for the fundus camera since the orientation rarely shifted much. The same cannot be assumed for the handheld fundus camera in which the shooting angle can change. This type of camera could produce tilted or misalign images. Fig.2 shows an example of a handheld fundus camera.

Figure 1.2 A mobile phone fundus camera [1]

[1] http://beaumontvision.com/introducing-the-peek-vision-smartphone-app/

Additionally, the cases of abnormal fundus image due to eye diseases provide challenges in determining the correct OD location. Fig.3 (left) represents a normal fundus image without any abnormal eye condition. The major retinal components are noticeable. This kind of image does fairly well with most of the algorithms proposed. Nonetheless, Fig. 3 (middle) and (right) can cause errors in OD localization. These kinds of images are problematic due to the presence of pathogen or diseases that alter the appearance of the OD making it difficult to determine its location. Fig. 3 (middle) represents an abnormal fundus image with bright lesion and Fig. 3 (right) represents an abnormal image with faint optic disc.

Figure 1.3 Examples of the abnormal fundus images

1.3 Purpose of study

The purpose of this study is to improve the accuracy and time of an existing method, the rotational 2D vessel projection, proposed by Tangseng's *et al.* and also overcome problems of incomplete network that it usually fails. In addition, we also look for ways to increase the robustness and accuracy of the algorithms to be able to adapt to different kind of images such as those with poor illumination and misshape OD.

1.4 Arrangement of thesis

The thesis is organized as follows: In chapter 2, related theories and the existing methods for locating the OD are presented. In chapter 3, methodology of Rotational 2D Vessel Projection with Decision Tree Classification and Circular Hough Transform with KNN classification are presented. Chapter 4 contains experimental setup, result and discussion of the proposed methods. Conclusion and recommendation are in chapter 5, followed by references, and list of my publication. MATLAB source code of Rotational 2D Vessel Projection with Decision Tree Classification is in Appendix A.

Chapter 2

Literature Review

This chapter described the existing methods of optic disc detection.

2.1 Projection of Image Features

Mahfouz's *et al.* [3] proposed the fast localization of the optic disc using projection of image features. They found that the current techniques used for locating the OD have problem with high computation time. Their technique required less than a minute to locate the OD. It works by searching the fundus image in one dimension projections encoding the *x* and *y* coordinates instead of searching in the two dimensional space. They obtain two significant 1D signals which can be used to locate the horizontal and vertical location of the OD. In order to obtain these signals, two features of the OD are exploited.

The first feature is about the blood vessel. We know from observation that the central artery and vein emerge mainly in the vertical direction and branch into the horizontal direction. Thus, the horizontal blood vessel would be dominated by the vertical when placed near the OD. The second feature relates to the intensity profile of the OD. We define the region of the OD as an area that is brighter than its surrounding.

In order to archive the 1D search space, the process is divided into 2 steps where two features map are constructed. In the first step, a horizontally sliding window as shown in Fig. 4 is construct by projecting the image feature onto the horizontal axis. The second step involves searching that given area for the vertical location of the OD. More details of each step will be covered below.

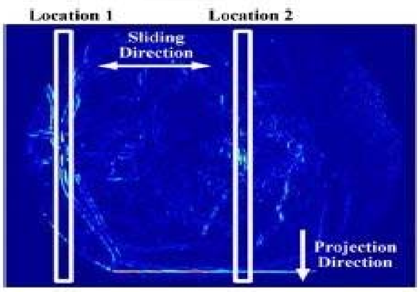

Figure 2.1 Illustration of horizontal sliding window

Horizontal Localization

The horizontal sliding window is construct by setting the width and height equal to twice the thickness of the main vessel. The window as shown in Fig.4 can then be used to scan across the image from left to right. For example, from location1 to location2. The differences between the vertical and horizontal blood vessels are computed. The window will encounter more vertical edges compare to the horizontal edges when placed near the OD. The maximum peak signal can be identified as the horizontal location of the OD as shown in Fig.5.

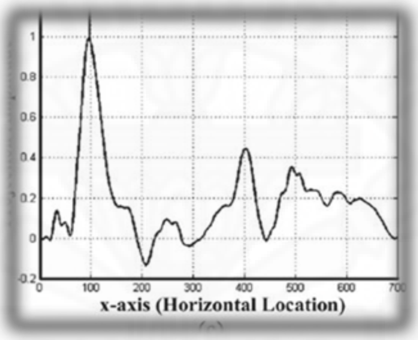

Figure 2.2 Illustration of 1D signal of horizontal axis

Vertical Localization

For the second step, the goal now is to search for the vertical location of the OD. We specify the vertical sliding window with the width and height equal to the OD's diameter and place it in the center of the horizontal sliding window we got from the previous step. The vertical location of the OD can then be determined by scanning the window from top to bottom along with projecting the image features onto a vertical axis. This is in order to create the second 1D signal. In normal fundus image, the number of bright pixels will increase when the window is center at the OD. Also, a large number of vertical and horizontal edges can be detected. The other locations apart from the OD will contain less edges and fewer bright pixels.

To improve the robustness of this method, they use weighting factors such as the geometric and appearance properties of the OD to select the location from a list of possible horizontal OD locations. This is because the maximum peak would not always indicate the right location of the OD. For example, other artifact or pathogen that causes brightness. They calculate the scoring index by multiplying the peak of the horizontal signal by the weighing factors.

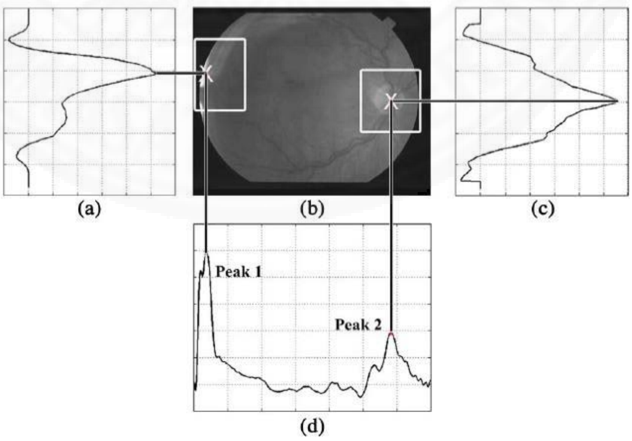

Figure 2.3 List of Possible OD Locations

2.2 Directional Models

Knowing the characteristic of retina vessel network and its convergence point, Wu *et al.* [1] proposed the technique of mapping a parabolic shape onto the main blood vessel of the fundus image. They made use of the 3 typical characteristics of OD which includes the gateway of the entire vessel network, the junction points of all the vessels, and the shape of a bright circular object. These characteristics give us an idea about the direction of vessels and the OD's intensity. Their model can be viewed as separated categories. The local directional model deals with the area around and within the OD. It exploits the characteristic of shape, brightness, and convergence of vessels to compute the gradient vector fields.

Otherwise, if the region of interest is defined to be the whole fundus image, it will be call a global direction model [1]. The latter model is considered to be robust against pathologies due to its high stability of vessel network. A pattern can be recognized when inspecting the fundus image from the global directional model. The vessel networks coming out of the OD tends to go in the same direction in which some will diverge into an area called the temporal region. The vessels from one side of the OD will bend toward the fovea. The other will diverge into to an area called the nasal region. The shape of the vessels can be approximately observed as a parabolic curve. The location of the OD is estimated to be the vertex of the curve. A global bi-parabola directional model (BPDM) is used to represent the whole vessels direction where a common vertex in the OD are share. We also assume that the opening angles of two parabolas matches and share the same horizontal symmetry axis. The last model, hybrid, is then used to pinpoint the OD locations by integrating results from both global and local models.

The following existing methods employ the concept of directional model:

2.2.1 Vessel Transform

Muangnak *et al.* [2] proposed the method called Vessel Transform (VT) to localize the OD by grouping the blood vessels into cluster. Segmentation algorithms are the key components used to calculate the OD location. To define the convergence region, one cluster is eliminated at a time from the list of found clusters.

The threshold is used as a way to accept vessel. It must meet the minimal length and thickness requirements. The retinal image goes through the process of vessel selection, clustering, and transform as well as median filtering and blob selection using SS to determine the OD location. If the convergence region is enclosed inside the contour, it's considered as a correct location. There are still cases where this method returns a mislocated OD due to too few clusters, too many incorrect vessel clusters due to vessel's segmentation algorithm. Moreover, despite the high accuracy, it suffers from slow running time.

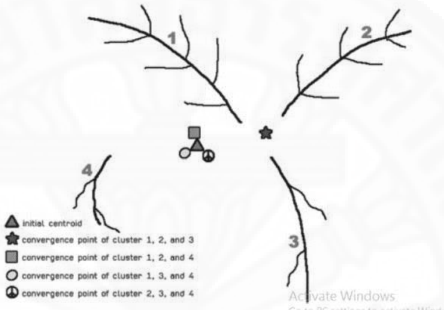

Figure 2.4 Convergence Region from Vessel Transform [2]

2.2.2 Rotational 2D Vessel Projection

Inspired by Mahfouz's algorithm, Tangseng *et al.* aim to pinpoint the OD location at any given angle of the input fundus image. He proposed the technique called Rotation 2D Vessel Projection (RVP) which solves the problem of disorientated image cases. By applying Mahfouz's technique each time the image is rotated by a small degree, the OD location can be projected. To rotate the original image to the new image at a clockwise angle, bilinear interpolation is used to perform a geometric transform. The final OD's location can be summarized from the overlapping of the tentative OD coordinates. Fig. 8 represent each of the processes in RVP. This method is suitable especially with images taken from handheld fundus camera since the orientation does not matter. However, its accuracy is uncertain in some abnormal OD cases.

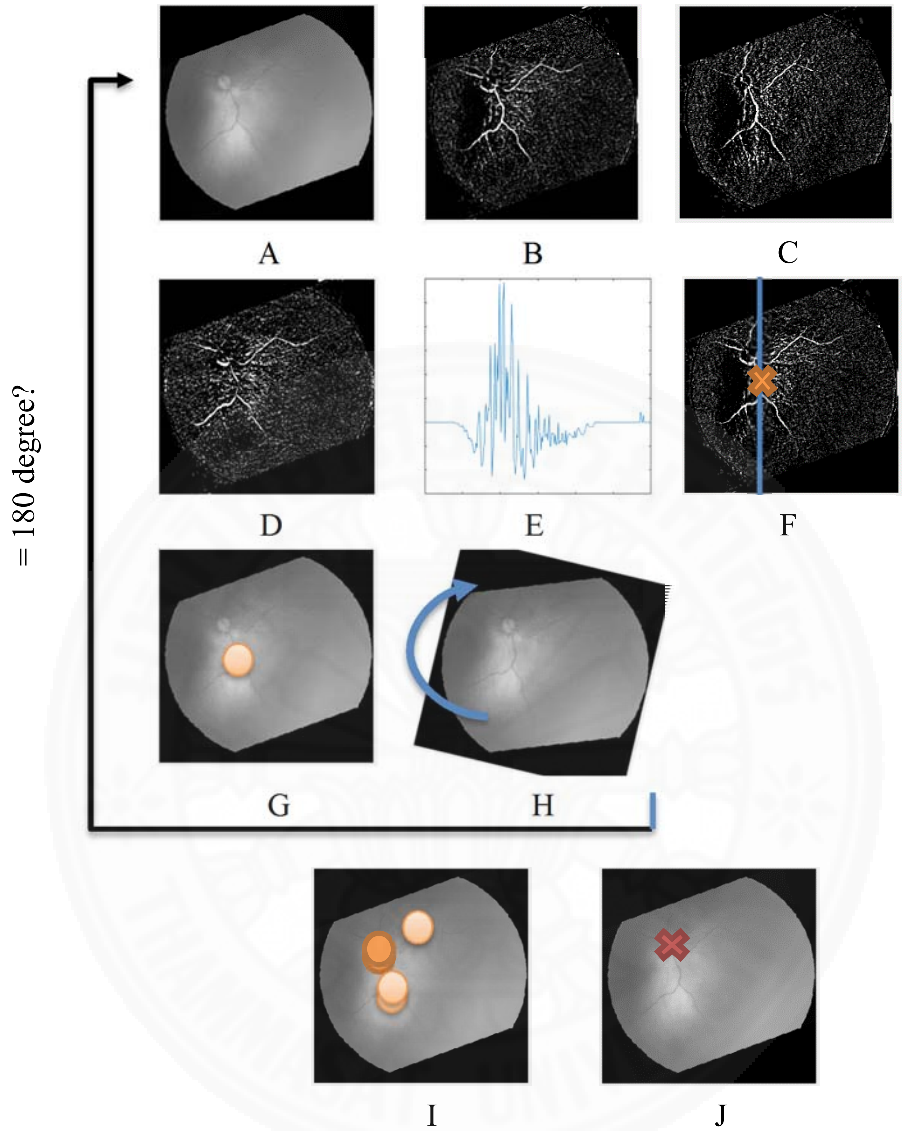

Figure 2.5 Illustration of processes in the RVP where (A) is the input grayscale image from ROP (20 degree) and (B) is the vessel image. (C) and (D) are vessel images extract from vertical and horizontal directions. The peak of the maximum difference between the numbers of vessels from both orientation (E) is set as the x's location. Mark down the brightest area at the given x's location (F) and (G). Rotate the input image by a small degree (H) and start the process again. The result from overlapping of OD coordinates (I) as voting scores and the final result (J).

Chapter 3
Methodology

3.1 Rotational 2D Vessel Projection with Decision Tree Classification

The overview of the proposed method will proceed in the following stages. At first, the input fundus image is converted into a grayscale image. This is in order to make the segmentation of blood vessels more precise. We use a top-hat filtering on complement of grayscale image to extract the blood vessels. To measure the threshold value of intensity, Otsu's *et al.* [6] is applied. The output image is then converted into a binary vessel image. Based on the input fundus image angle, we develop an algorithm to rotate the image by t degree per step. The value of t in the range of 5 to 15 is adequate for our implementation. For each degree, we apply Mahfouz's method to get the X's location of the OD. This is done by calculating the differences in the number of vessel pixels in the horizontal and the vertical position obtained through a morphological opening. The equation describing this can be view as

$$x_{loc} = \underset{x}{\operatorname{argmax}}\, V(x) - H(x)\,, \qquad (1)$$

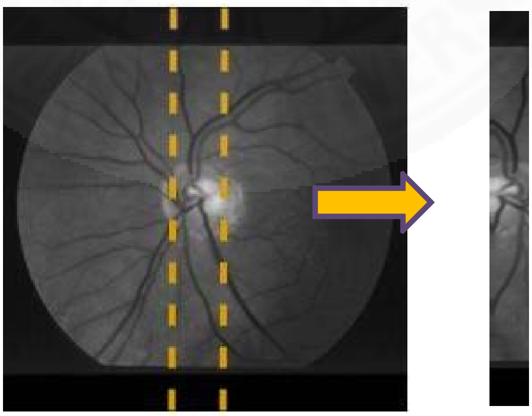

Figure 3.1 Section of the sliding window

We then use that location per each degree to extract a vertical stripe dimension *w* by *h* running down from the top to the bottom where h is the height and w is the width of the stripe. Sliding window is used for both features extraction and classification to select the Y's location candidates. This is made possible with the prebuild decision tree classification model attained from comparing between OD features and the ground truth.

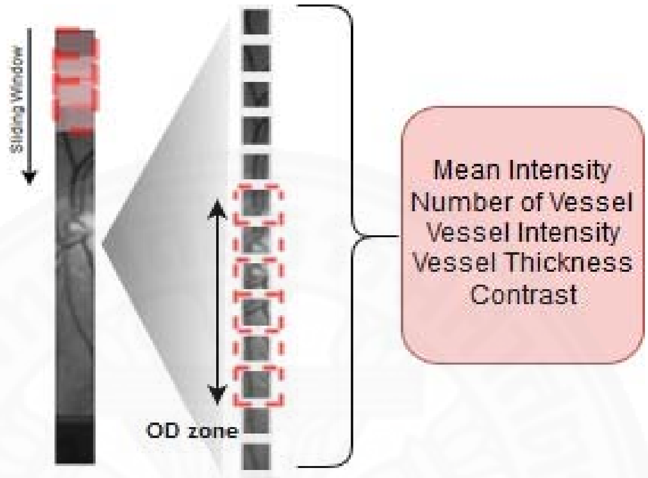

Figure 3.2 X Image of sliding window

Some section of the windows can be seen in Fig. 9 where the OD are marked with red frames and the rest are non-OD. In the case that there are multiple windows selected as the Y's candidates, the window at the center is concluded to represent the OD location. Before the iteration ends, we mark down a circle on a separate canvas given both X and Y coordinates. The circle fitted to the selected window, in all pixels, is given a voting score of 1. Finally, we rotate the image with an incremented t degrees and repeat this process from 0 to 180 degree. The area with the most score is selected as the final OD's region after we reach 180 degree which is the maximum rotated angle. Fig. 10 describes the conceptual model of this work. Fig. 11 shows the flowchart of finding the final OD's location. Fig. 12 illustrate the processes in RVPDT when the original image is tilted by 45 degree.

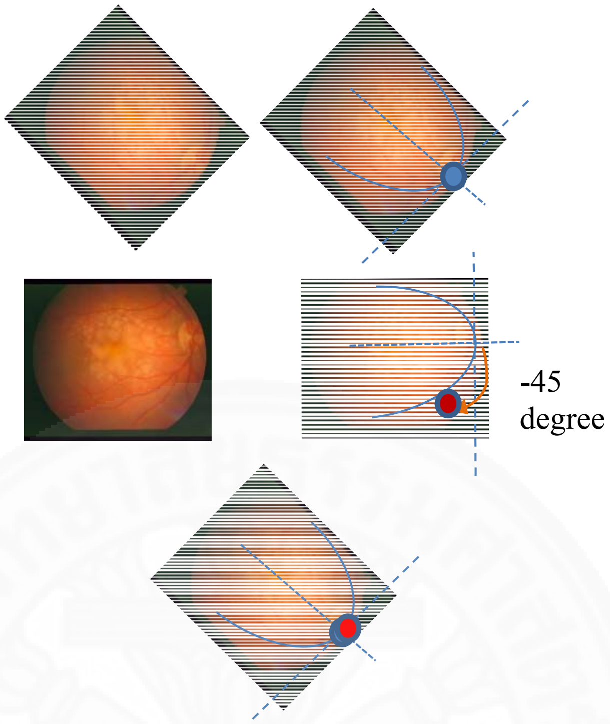

Figure 3.3 (top-left) tilted image and (top-right) the parabola fitting the vessels of this tilted image. (middle-left) image shifted by 45 degree counter clockwise and (middle-right) its the parabola fitting the vessels. (bottom) the overlay of the OD locations at -45 degree and OD location obtained at 0 degree and then shifted by.

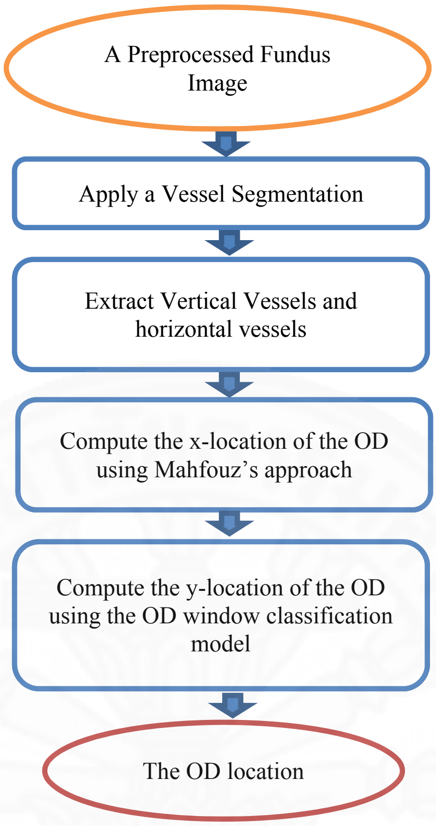

Figure 3.4 A flowchart depicting procedures of OD localization of the Mahfouz-DT approach

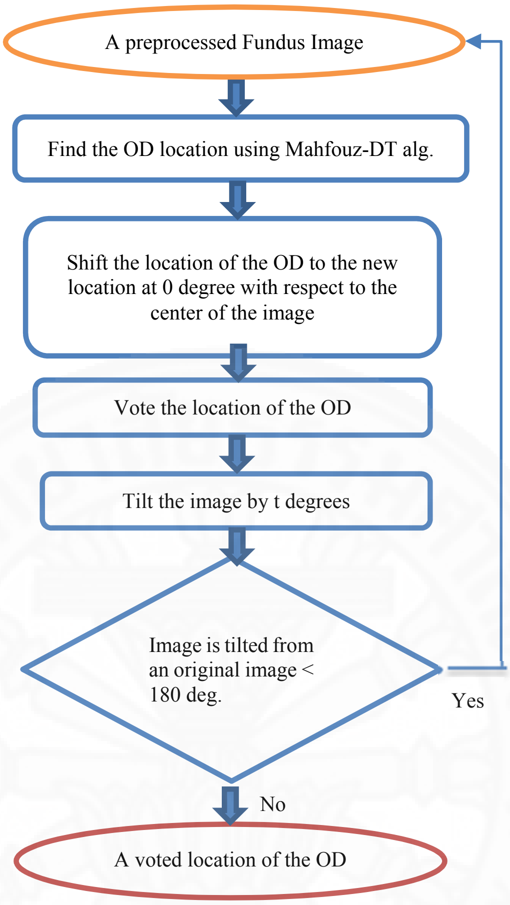

Figure 3.5 The flowchart illustrating overview of the proposed RVPDT method

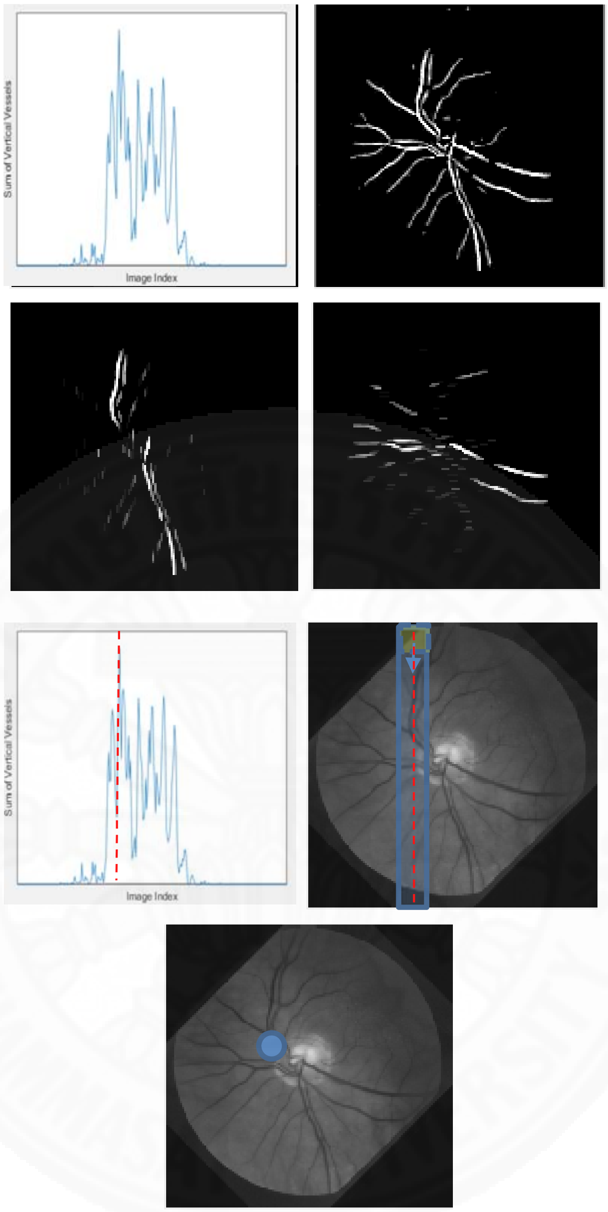

Figure 3.6 Illustration of processes in the RVPDT where (top-right) is the input grayscale image from STARE (45 degree) and (top-left) is the vessel image. (middle-left) and (middle-right) are vessel images extract from vertical and horizontal directions. The peak of the maximum difference between the numbers of vessels from both orientation (bottom-left). The classification is performed on the focused zone (bottom-right). The final concluded OD location (bottom).

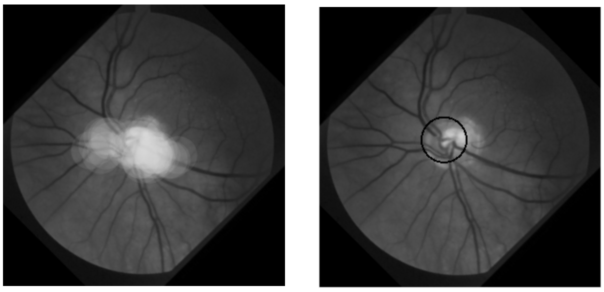

Figure 3.7 X Image of overlapping location collected from each iteration at different degrees (left) and the final OD location obtained from the proposed method (right).

In total, there are 5 features collected from each window for the classification stage which includes the mean intensity, the number of vessels, the vessel intensity, the image contrast, and the vessel thickness. In order to collect these statistic, we apply a sliding window to scan the obtained x location bar from the top to the bottom. Each window from the bar will give 5 features. The example of the training data can be seen in Table 3.1. We feed in all of these instances to the pre-constructed decision tree model in order to select the windows which is most likely to be the OD. There will probably be more than one windows selected as the candidates. However, only the median among those candidates is finalize as the index of the final OD location.

Once the final OD window is determined, a circle with a radius approximately one sixth of the diameter of the retina is plotted on to a new canvas using both x and y coordinates. We set the region of circle to have a low value of intensity. This way when the circles are placed on top of one another, the intensity value can be accumulated and used as a voting score. After the rotation is complete, we will end up with circles of OD candidates. Fig. 13 displays an overlapping of circles obtained when the rotation is complete. The final OD location is selected as an area with the most overlying of circles.

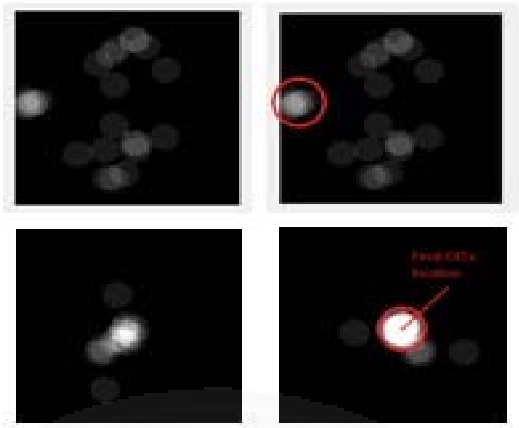

Figure 3.8 Overlapping of circles on canvas. The brightest area is the location where the circles are overlapped the most.

Machine learning is utilized to make the comparing phase possible. We trained each data set beforehand using the Matlab's decision tree classification. In the case of STARE and ROP, we chose images that follows the assumption that the vessels are not misalign. We run the program from these kind of images, including both fair and poor groups, for the sole purpose of gathering instances. The ground truth is used to mark windows that are associated with the OD. This produces an extra column in the matrix. Given 168 instances per image, there will be a total of 11340 instances for STARE dataset and 12740 instances for ROP dataset. After all the instances are collected, the ground truth value of the OD is set as a response whereas the rest is set as predictors.

There are two types of validation method which are cross validation and holdout. We selected cross validation with 10 folds to divide and test the data. Each fold is divided into two groups of training and testing.

When we first tested the instances, we tried to adjust the data by balancing out the number of 0s and 1s which corresponds to OD and non-OD. This results in discarding a lot of non-OD instances in an attempt to reduce the false positive error. Nevertheless, the accuracy from the trained model is lower so we return to use the data without adjustment.

There are several data classification techniques available. The decision tree's confusion matrix has the highest percentage of accuracy. The model can then be built and combined to our program.

Table 3.1 Examples of training Data

Mean Intensity	Vessel Number	Vessel Intensity	Vessel Thickness	Contrast	isOD
120	3	2032	0.7	130	0
126	3	2185	1.1	156	1
155	2	31248	1.9	215	1
131	8	3582	1.4	177	0

As RVPDT assumptions primarily depend on the structure of the main vessels in order to determine the OD's x location, a partial or an incomplete curve of the vessel can ruin the result completely. We aim to improve on the existing RVPDT's OD localization method by examining the failed cases. The next method is proposed to solve such cases.

3.2 Circular Hough Transform with KNN Classification

The proposed Circular Hough Transform with k-nearest neighbor (KNN) classification method is derived from the physical appearance of the fundus image. There are many reasons which explain why the structure of the blood appears to be incomplete. Most of them are linked to the segmentation process. As in the cases when the illumination of the input image is simply too dark or too bright, they become problematic to distinguish the vessels from the background as shown in Fig.14. This also includes cases with thin or faint vessels. Another reason is related to the assumption that the fundus's main vessels resembles a parabola shape and the OD is located at the vertex. This, however, does not apply to all cases. Some fundus's vessel structures simply do not merge at the vertex or the OD can appear elsewhere along the vessel structure.

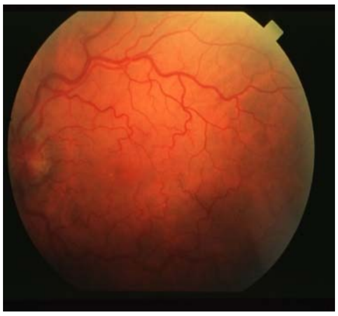 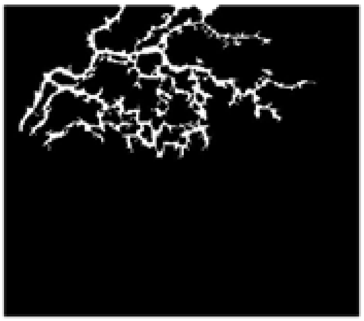

Figure 3.9 An example of image with uneven illumination

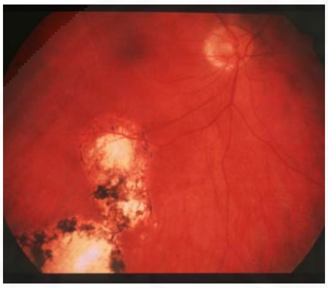 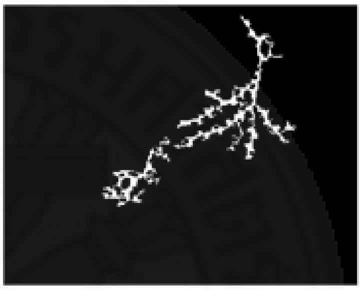

Figure 3.9.1 An example of a vessel an incomplete parabola

Given the above observations, we derived a method to complete the missing network of the main vessel structure to scan for the OD using circular Hough transform. Circular Hough transform is a feature extraction technique used for detecting circular objects in digital images [14]. The reason we preferred circles rather a parabola is because the parabola's vertex cannot simply be determined. There could be several parabolas with different vertexes in many angles when compared to a complete circle. Moreover, a fact that the tails of the parabola normally shown as thin and faint vessels are not very important information, when focus on only main vessels which are thick and dark , the shape of the structure of the main vascular network is closer to the circle.

The overview of this algorithm will proceed in the following stages. At first, the input fundus image is converted into a grayscale image in order to segment the blood vessels. During the segmentation process, we applied a threshold value of minimum thickness to eliminate small branches and spikes erupted from the vessels which are considered as noises. Second, we extracted the *n* largest connected components from the binary vessel image to select only the main parts of the vessel structure where n is arbitrary number. This is derived from the observation that the main vessel structure is thicker than its branches. The value of *n* is dependent to the fundus dataset, for instance, STARE requires less than ROP. Next, the circular Hough transform is applied to loop thorough all the pixels from the segmented image. From observation, we specified a certain range of radius which would be suitable for Hough to iterate and fit a curve to. It selects the circle candidates by voting among the local maxima. To increase the accuracy, we fitted two separated circles to increase the possibility that the main structure is mapped and intersected with the OD. The neighborhood suppression method will ensure us that the two circles are spatially separated.

To conclude the final OD location, we consider series of moving windows similar to the previously proposed RVPDT techniques. This time it moves along a circular trajectory coordinates extracted from the mapped circles. A filter is applied to only consider windows that have a certain number of vessels. This will reduce the machine learning's search space by cutting the quadrants that are not related to the OD. The KNN classification model obtained from the ground truth are tested on to these moving windows to find windows that contain the OD. It works by using a distance function to get the k nearest neighbors and average their weight to perform regression. When there are multiple windows having OD, the median of these windows is selected to represent the OD location. Given that we selected two separated circles of best fit, the sliding window will move along both of them to gather the features instances. In the case that KNN classification picked windows from two different circles, the average intensity among these windows will be compared. Window which gives a higher value will represent the final OD location.

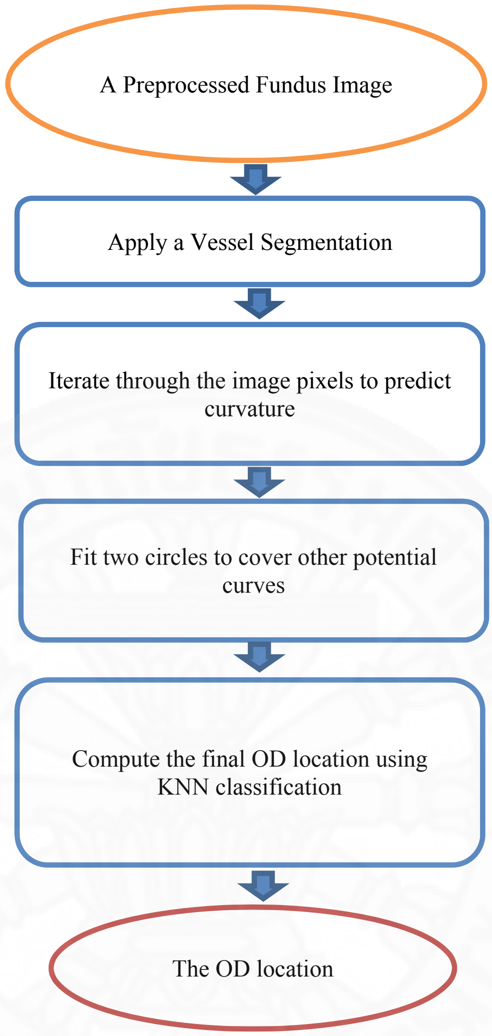

Figure 3.9.2 A flowchart depicting the CH-KNN algorithm

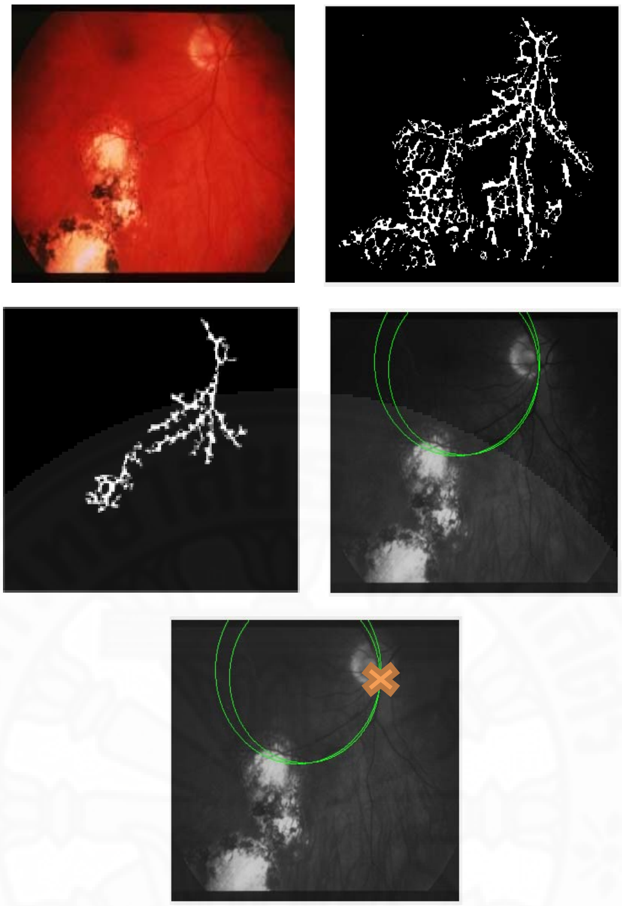

Figure 3.9.3 Illustration of processes in the CH-KNN where (top-left) is the input image and (top-right) is the vessel image. (middle-left) is the vessel images after selected the most connected components. (middle-right) is the result after applying circular Hough to map two circles. The classification is performed on two of the focused trajectories (middle-right). The final concluded OD location colored red (bottom).

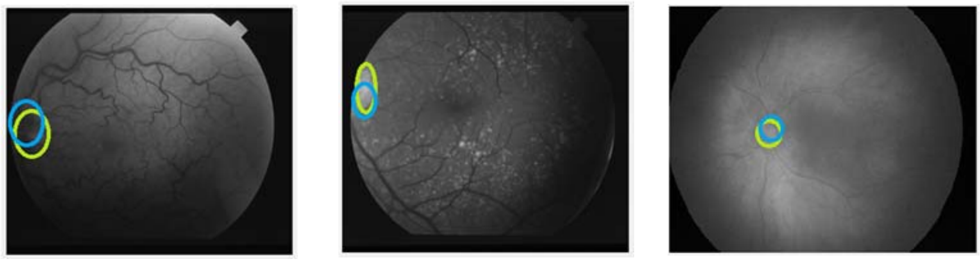

Figure 3.9.4 Examples of OD localization using CH-KNN on incomplete vessel images, blue outline-CH-KNN, green outline– ground truth

3.3 Experimental setup

The proposed Rotational 2D Vessel Projection with Decision Tree Classification (RVPDT) and Circular Hough Transform with KNN Classification are used to evaluate the accuracy in locating the OD from the Structured Analysis of the Retina (STARE) and retinopathy of prematurity (ROP). The former set are given by the Shiley Eye Center at the University of California, San Diego, and by the Veterans Administration Medical Center in San Diego. These images have a same resolution of 700 by 605 pixels. Each of the dataset are separated into two groups of fair and poor groups. Fair images represent the healthy eye condition with a clear boundary of the ODs. The background lighting is distributed evenly and blood vessels are not fade. Poor image represent an unhealthy eye condition with an unclear boundary of the OD. They are difficult to deal with because the images can contain several abnormalities from certain eye conditions that alter the appearance of the OD. The OD can even loss its circular shape or its brightness. In some severe cases, they are not unrecognizable even with a naked eye.

3.3.1 Setup for RVPDT

To validate the performance of our algorithm for each datasets, we test the images from different starting angles. This process is necessary as it emulates the input data from rotated images. During the pre-processing phase, the fundus images are rotated to 13 angles including 0, 15, 30, 45, 60, 75, and 90, 105, 120, 135, 150, 165, 180 with an increment of 15. Bilinear interpolation are used to perform a counter-clockwise rotation. We evaluate our algorithm's performance against Mahfouz's *et al.* [3] and Tangseng *et al. [5]* in 13 starting angles.

The first dataset named STARE has a total of 81 images. It is separated into 31 fair images and 50 poor images. The second dataset named ROP has a total of 91 images. It is consisted of 60 fair images and 31 poor images. The algorithm is tested on different starting angles range from 0 to 180 degree. RVPDT is implemented and executed using MATLAB running on a Microsoft Windows 8 laptop with Intel Core i7-4510 @ 2.00GHz and 4GB of RAM.

3.3.2 Setup for Circular Hough Transform with KNN Classification

To validate the performance of our algorithm for each datasets, we test the image against Mahfouz's *et al.* [3] , Tangseng *et al. [5]* , and RVPDT without rotating the input fundus image.

The first dataset named STARE has a total of 81 images. It is separated into 31 fair images and 50 poor images. The second dataset named ROP has a total of 91 images. It is consisted of 60 fair images and 31 poor images. CH-KNN is implemented and executed using MATLAB running on a Microsoft Windows 8 laptop with Intel Core i7-4510 @ 2.00GHz and 4GB of RAM.

Chapter 4

Result and Dicussion

4.1 Result and discussion of RVPDT

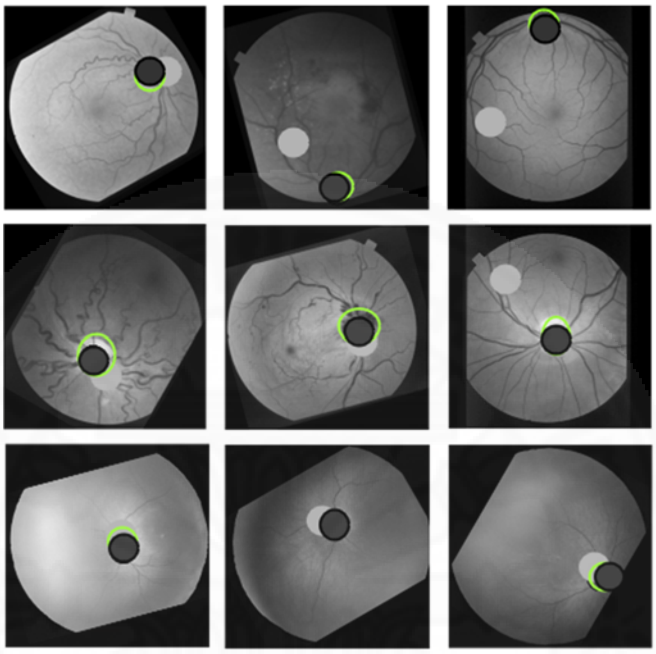

Figure 4.1 Example of OD Localization: **black circle - our result, grey circle – Mahfouz, green outline – ground truth**

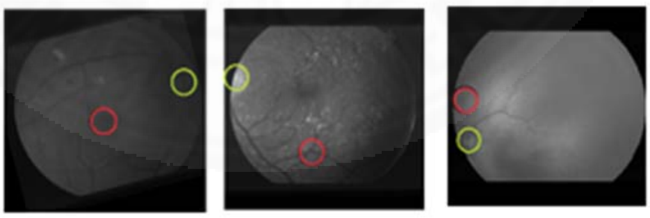

Figure 4.2 Example of unsuccessful OD Localization**, red outline- our result, green outline– ground truth**

The result of STARE and ROP datasets can be seen in Fig. 20 and Fig. 21. The successful cases of OD localization from different starting angles are shown in Fig. 20. Fig. 21 represents the fail cases. The first two cases of Fig.21 are caused by poor background illumination. It is difficult to identify the fundus features in these type of images. The last fail case is the one from premature fundus. The number of vessels is not enough to predict the OD location precisely. There are numbers of way which could lead to improvements such as developing an enhanced algorithm to be able to determine the value of image features from poor environment or a segmentation algorithm which is capable to detect and eliminate distraction from uneven background.

RVPDT produced an accuracy of 86% for STARE dataset and 76% for ROP dataset. It takes about 13 seconds per image to pre-process and localize the OD. The total computation time does not include the time to prepare the training model. The evaluation between Mahfouz's *et al*. [3], RVP of Tangseng *et al.* [5] and our RVPDT performance on STARE and ROP datasets are shown is Table 4.1.

4. 2 Result and discussion of CH-KNN

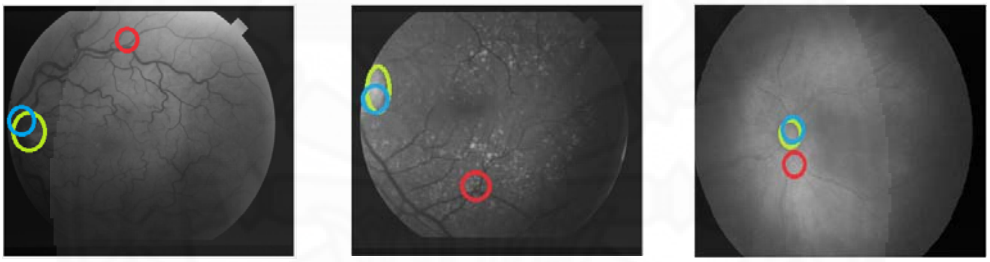

Figure 4.3 Example of successful cases against RVPDT**,** red outline- RVPDT result, blue outline-CH-KNN, green outline– ground truth

Some results of STARE and ROP datasets against RVPDT can be seen in Fig. 22. The left image represents a bad background illumination. The middle image represent the missing vessel structure. Both of these images are from STARE. The right image is from ROP where RVPDT barely missed the ground truth.

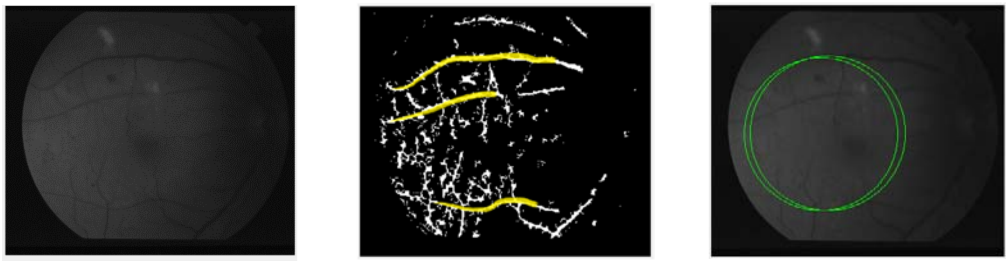

Figure 4.4 Illustration of an unsuccessful case of CH-KNN where (left) is the input greyscale. (middle) represent the vessel image and (right) is the result of Hough transform

There are image cases that Hough fail to locate the OD correctly. One example is shown in Fig. 25 where the input image has a poor background illumination. When we try to complete the missing vessel structure, the circles are mapped to the wrong curvature. This is due to the segmented vessel image containing wave like lines highlighted in yellow that mislead the algorithm. Thus, none of the windows are selected by the classification model.

CH-KNN produced an accuracy of 87% for STARE dataset and 80% for ROP dataset. It takes 8 seconds per image to pre-process and localize the OD. The total computation time does not include the time to prepare the training model. The evaluation between Mahfouz's *et al*. [3], Tangseng *et al.* [5] , RVPDT and CH-KNN performance on STARE and ROP datasets are shown is Table 4.2.

Table 4.1 The Accuracy of OD Location

Collections	Tilt angle	Avg. Accuracy, %		
		Mahfouz	RVP	RVPDT
STARE	0	72	70	86
	15	70	78	86
	30	65	77	85
	45	52	78	81
	60	32	73	85
	75	23	78	90
	90	21	73	84
	105	33	78	88
	120	40	73	86
	135	60	73	85
	150	69	73	88
	165	72	73	85
	180	73	70	86
	Avg	**52**	**74**	**86**
ROP	0	51	71	75
	15	53	74	79
	30	53	70	70
	45	51	74	75
	60	44	70	77
	75	35	79	81
	90	30	72	74
	105	38	69	78
	120	47	76	76
	135	57	79	77
	150	57	75	81
	165	51	74	76
	180	46	71	75
	Avg	**47**	**73**	**76**

Table 4.2 The Accuracy of OD Location

Collections	Avg. Accuracy, %			
	Mahf ouz	RVP	RVPDT	CH-KNN
STARE	72	70	86	**87**
ROP	51	71	75	80

Chapter 5
Conclusions and Recommendations

In this work, we proposed two algorithms of OD localization. The first is an automated fast, robust, and accurate method by integrating machine learning to identify the OD location. The second named circular Hough transform with k-nearest neighbor's classification, CH-KNN, is an automated fast and accurate algorithm utilizing machine learning as well as curve mapping to identify the OD location. A combination of OD features such as the vessel intensity, vessel number, image contrast, mean intensity, and vessel thickness are collected during the process of both methods. RVPDT is versatile to all orientation of the input fundus image since it involves image rotation. CH-KNN provides a solution to an uncompleted network of vessel.

Despite the high accuracy of both algorithms, there are still rooms for improvements. Both algorithms could use better ways to collect the fundus image features that are unaffected by abnormal eye conditions. It is also possible to increase the number of features apart from the mentioned ones.

References

1. X. Wu, B. Dai, W. Bu, "*Optic Disc Locatization Using Directional Models*"IEEE Trans. Image Process,.,vol 25, no. 9, pp 4433-4442, July 2016
2. N. Muangnakm, P. Aimmanee, S. Makhanov, B. Uyyanonvara,"*Vessel transform for automatic optic disk detection in retinal images*" IET Image Process., vol. 9, no.9, pp.743-750, Aug 2015
   A. E. Mahfouz and A. S. Fahmy, "*Fast Localization of the Optic Disc Using Projection of Image Features*" IEEE Trans. Image Process., vol. 19, no.12, pp. 3285-3289, Dec.2010
3. Q. Cao, J. Liu, Q. Zhao., "*Fast Automatic Optic Disc Localization in Retinal Images"*, Image and Graphic (ICIG), 2013 Seventh International Conference on, vo1., pp. 827,831
4. P. Tangseng, "*Rotational 2D Vessel Projection*" Sirindhorn International Institute of Technology Thammasat University, 2014
5. Otsu, N., "A Threshold Selection Method from Gray-Level Histograms," *IEEE Transactions on Systems, Man, and Cybernetics*, Vol. 9, No. 1, 1979, pp. 62-66.
6. D. Zhange, Y. Zhao " *Novel Accurate and Fast Optic Disc Detection in Retinal Images with Vessel Distribution and Directional Characteristic*,"IEEE J. Biomed. Health Informat., vol.20, no. 1,pp. 333-340, Jan.2014
7. Burk, Scott, John S. Cohen, and Harry Quigley. *Healthy Optic Nerve and Optic Nerve in Eye with Glaucoma*. Digital image.Optic Nerve Cupping | Glaucoma Research Foundation. Glaucoma Research Foundation, 21 Aug. 2012. Web. 19 May 2015.
8. Normal Vision and the Same Scene as Viewed by a Person with Glaucoma. Digital image. Facts About Glaucoma | National Eye Institute. The National Eye Institute (NEI), n.d. Web. 19 May 2015.
9. S. Lu, J. Liu, J.H. Lim, Z. Zhang, N.M. Tan, W.K. Wong, T.Y. Wong. (2010). Automatic optic disc segmentation based on image brightness and contrast, *In SPIE Medical Imaging, International Society for Optics and Photonics 76234J*(2010) 1-8.
10. Michael Goldbaum. (2003). *The STARE Project*, from http://www.ces.clemson.edu/~ahoover/stare/
11. Normal Vision and the Same Scene as Viewed by a Person with Glaucoma. Digital image. Facts About Glaucoma | National Eye Institute. The National Eye Institute (NEI), n.d. Web. 19 May 2015.
12. J.J. Staal, M.D. Abramoff, M. Niemeijer, M.A. Viergever, B. van Ginneken,

"Ridge based vessel segmentation in color images of the retina", *IEEE Transactions on Medical Imaging*, 2004, vol. 23, pp. 501-509.
13. J. Illingworth and J. Kittler, “The Adaptive Hough Transform,” PAMI-9 , Issue: 5, 1987, pp 690-698

PUBLICATION

B. Sutcharit, P. Aimmanee, P. Tangseng, (2018). OD Localization Using Rotational 2D Vessel Projection with Decision Tree Classification. 27-32. 10.1145/3193063.3193075

Appendix

APPENDIX A

Rotational Vessel Projection with Decision Tree Classification MATLAB source code

```
%Rotational Vessel Projection
    [maxy,maxx] = size(img);
    difxy = abs(maxx-maxy);
    side = max(maxx,maxy);
    sqImg = zeros(side,'uint8');
    addSp = round(difxy/2);
    if(maxx > maxy)
        if(mod(difxy,2)==0)
            sqImg([addSp+1:side-addSp],:) = img;
        else
            sqImg([addSp:side-addSp],:) = img;
        end
    else
        if(mod(difxy,2)==0)
            sqImg(:,[addSp+1:side-addSp]) = img;
        else
            sqImg(:,[addSp:side-addSp]) = img;
        end
    end
    maxx = side;
    maxy = side;
    img = sqImg;
    maxThick = 6;

    %
=========================================================
=========================================================
==============
    img = imrotate(img,startingAngle,'bilinear','crop');
    rotatedGT =
imrotate(GT,startingAngle,'bilinear','crop');
    [bwImg,filteredImg,sdMap,vLog] =
seg_exp(img,maxThick,3);

=========================================================
=========================================================
==============
    score = intmax();
    ansCount = 0;
    cAngle = 0;
    ODR = 25;
    step = 5;
```

```
    baseBwImg = bwImg;
    baseImg = img;
    outImg = zeros(maxy,maxx);
    outImg2 = zeros(maxy,maxx);

    for i=0:180/step
        angle = i*step;
        bwImg =
imrotate(baseBwImg,angle,'nearest','crop');
        img = imrotate(baseImg,angle,'nearest','crop');
        outImg = imrotate(outImg,angle,'nearest','crop');
        outImg2 =
imrotate(outImg2,angle,'nearest','crop');

        [height,width] = size(bwImg);
        [x,diff,bwH,bwV] = fastXPos(bwImg,maxThick);

        imGray = img;
        imNoV = removeVessel(imGray,bwImg);


                [croppedImage1,croppedvImage1] =
learnY(outImg,img,bwImg,x);
            [y] =
learnYbar(croppedImage1,croppedvImage1);

        outImg2 = fillCircle(outImg2,1,x,y,ODR);

        mid = maxy/2;
        % Draw a filled circle at OD
        outSingle = zeros(maxy,maxx);
        outImg = imrotate(outImg,-
1*angle,'nearest','crop');
        outImg2 = imrotate(outImg2,-
1*angle,'nearest','crop');
    end


%Feature Extraction and Classification
function [y] = learnYbar(cropImg,cropvImg)
    [row_cropped col_cropped] = size(cropImg);

    %301 21
    col_cropped = 21;
array1 = zeros(1,10);
array2 = zeros(1,10);
array3 = zeros(1,10);
array4 = zeros(1,10);
```

```
array5 = zeros(1,10);
array6 = zeros(1,10);
v = 0;

num_win = 30;
mymatrix = zeros(28,5);

rvImg = removeVessel(cropImg,cropvImg);
%figure,imshow(cropGT);
for i=0:27
    step_size = floor(row_cropped/num_win);
    topRow = step_size*i;

    if topRow == 0
        topRow =1;
    end

    win = cropImg(topRow:topRow+col_cropped, :);
    winrv = rvImg(topRow:topRow+col_cropped, :);
   % Mean Intensity -----------------------

    feature1 = mean(mean(win));
    array1(i+1) = feature1;

    win2 = cropvImg(topRow:topRow+col_cropped, :);

    % Number of Vessel ----------------------
    BW2 = bwmorph(win2,'skel',Inf);

   % white = sum(BW2(:));
    %feature2 = white;
    num = bwconncomp(win2);
    numves = num.NumObjects;
    feature2 = numves;
     array2(i+1) = feature2;

     % Vessel Intensity ------------------------
   if numves == 0
       VesIntensity = 0;
   else
       VesIntensity = sum(sum(win2))/numves;
   end
     feature3 = VesIntensity;
     array3(i+1) = feature3;

     % Vessel Thickness ----------------------
    s = regionprops(win2, 'MajorAxisLength',
'MinorAxisLength');
```

```
    if numel(s) == 0
        VesThickness = 0;
    else
        VesThickness = mean([s.MajorAxisLength
s.MinorAxisLength], 2);
    end

    %white = sum(win2(:));
    feature4 = VesThickness;

   array4(i+1) = feature4;

    % Contrast -------------------------------
    image_contrast = max(win(:));
    feature5 = image_contrast;
    array5(i+1) = feature5;

    % OD? ------------------------------------

    %win3 = cropGT(topRow:topRow+col_cropped, :);

  % OD = mean(mean(win3));
    %if (OD == 0)
       % feature6 = 0;
      %  v = v+1;
    %else
     %   feature6 = 1;
   % end
   % array6(i+1) = feature6;

     mymatrix(i+1,1) = feature1;
     mymatrix(i+1,2) = feature2;
     mymatrix(i+1,3) = feature3;
     mymatrix(i+1,4) = feature4;
     mymatrix(i+1,5) = feature5;
     %mymatrix(i+1,6) = feature6;


 %  warning('off','all');
   %figure(3),
  % subplot(20, 1, i+1);
          %imshow(win);
          %[o p] =size(win3);
          %disp(o);

end
```

```
        %header = {'x1','x2','x3','x4','x5'};
        %output = [header; num2cell(mymatrix)];

T =
array2table(mymatrix,'VariableNames',{'Mint','Vnum','Vint
','Vthick','Cont'});
%T =
array2table(mymatrix,'VariableNames',{'x1','x2','x3','x4'
,'x5'});

%[success,message] =
xlsappend('Pending.xlsx',mymatrix,'Sheet1');


      VarName = evalin('base','rop');
      %VarName = evalin('base','trainedClassifier1');
 yfit = VarName.predictFcn(T);
 inds = find(yfit==1);
 med = median(inds);
 med = med -1;

 topRow = step_size*med;
 bottomRow = topRow + col_cropped;
 y = (topRow + bottomRow)/2;
```